

Electron-induced stabilization of ferromagnetism in  $\text{Ga}_{1-x}\text{Gd}_x\text{N}$ 

Gustavo M. Dalpian and Su-Huai Wei

National Renewable Energy Laboratory, Golden, Colorado 80401, U.S.A

(Dated: March 23, 2024)

Using *ab initio* band structure calculations and symmetry arguments, we show that the magnetic property of  $\text{Ga}_{1-x}\text{Gd}_x\text{N}$  is drastically different from TM-doped GaN. The coupling between Gd atoms in the alloy is antiferromagnetic, but the ferromagnetic phase can be stabilized by introducing electrons. Furthermore, we propose a model that may explain the recently observed colossal magnetic moments in this system, based on the polarization of donor electrons.

PACS numbers: 75.50.Pp, 71.55.Eq, 71.70.-d, 71.20.Eh

## INTRODUCTION

The development of future spintronic devices will likely rely heavily on engineering materials that can have efficient spin injection into semiconductors at high temperature [1, 2]. Among the most promising candidates for this task are some diluted ferromagnetic nitrides and oxides, [3] which have small separation between magnetic ions and small spin-orbit coupling at the band edge. Most of the materials that have been studied are semiconductors doped with partially filled 3d transition metals (TMs). Because of the strong coupling between the magnetic ions' 3d states and the coupling to the host p states, diluted magnetic nitride and oxide semiconductors have been predicted and, in some cases, observed to show hole-mediated ferromagnetic behavior above room temperatures [1, 2, 3]. However, high  $T_c$  behavior of the 3d TM-doped nitrides and oxides is often impeded by the formation of precipitates [4] or compensated by n-type carriers that are intrinsic for these wide gap semiconductors [5, 6]. Recently, nitrides and oxides doped with partially filled 4f rare-earth (RE) ions have been proposed as an interesting alternative to achieve high  $T_c$  in these materials. Indeed, ferromagnetism has already been observed in  $\text{Ga}_{1-x}\text{Gd}_x\text{N}$ , with Curie temperature larger than 400 K [7, 8, 9].

Despite the partial success, the nature of the host-impurity couplings, and of the ferromagnetic interactions in  $\text{Ga}_{1-x}\text{Gd}_x\text{N}$  and other RE-doped nitrides and oxides, is not very well understood. On one hand, 4f orbitals are more localized, thus the direct coupling between the 4f ions is expected to be weak. On the other hand, 4f RE elements can have larger magnetic moments than the 3d elements, and, unlike the d states, f electrons can couple strongly with the host s electrons, leading to the possibility of electron-mediated ferromagnetism in these materials. Furthermore, colossal magnetic moments of Gd in GaN have been observed, which has a close connection to the observed ferromagnetism in this system [8]. But the origin of the observed colossal magnetic moments is not known.

To get a deep understanding of the nature of magnetic coupling in these RE-doped systems, in this work,

we perform total energy and band structure calculations of  $\text{Ga}_{1-x}\text{Gd}_x\text{N}$  for a few concentrations, including the hypothetical GdN in the zinc-blende structure. We show that the interactions between Gd atoms in undoped  $\text{Ga}_{1-x}\text{Gd}_x\text{N}$  are antiferromagnetic in nature, but this can be changed by introducing donors to the material; different from most 3d diluted magnetic semiconductors, ferromagnetism in  $\text{Ga}_{1-x}\text{Gd}_x\text{N}$  is electron-mediated [10], because the splitting of the conduction band, induced by the s-f coupling, is larger.

## METHODOLOGY

The total energy and band structure calculations in this study were performed using the general potential linearized augmented plane wave (LAPW) method [11] within the density functional theory and the local spin density approximation (LSDA) for the exchange-correlation potential. The muffin-tin (MT) radii are 1.48 Bohr for N, 2.50 Bohr for Gd, and 2.05 Bohr for Ga. The Gd 5p and Ga 3d semicore states are treated in the same footing as the other valence orbitals. The Brillouin-zone integrations were performed using a  $4 \times 4 \times 4$  Monkhorst-Pack special k-points [12] and equivalent k-points for the superstructures. We find that the LSDA-calculated lattice parameters for both GaN and GdN are in excellent agreement with experiment. Our calculated lattice parameters for GaN and GdN in the zinc-blende structure are 4.497 and 5.291 Å. The difference in the lattice constant between ferromagnetic (FM) and antiferromagnetic (AFM) configurations of GdN is less than 0.2%. It should be noted that pure GdN usually crystallizes in the NaCl structure. We calculated the lattice parameter of GdN in this structure, finding it to be 4.978 Å, which is in excellent agreement with the experimental value of 4.974 Å [13]. For the alloys, we assume that Vegard's rule is obeyed for the lattice constant, and the interatomic positions are fully relaxed by minimizing the total energy and quantum mechanical forces. In this work we study Gd incorporated in zinc-blende GaN and assume that the physical properties are similar for Gd incorporated in the more stable wurtzite GaN.

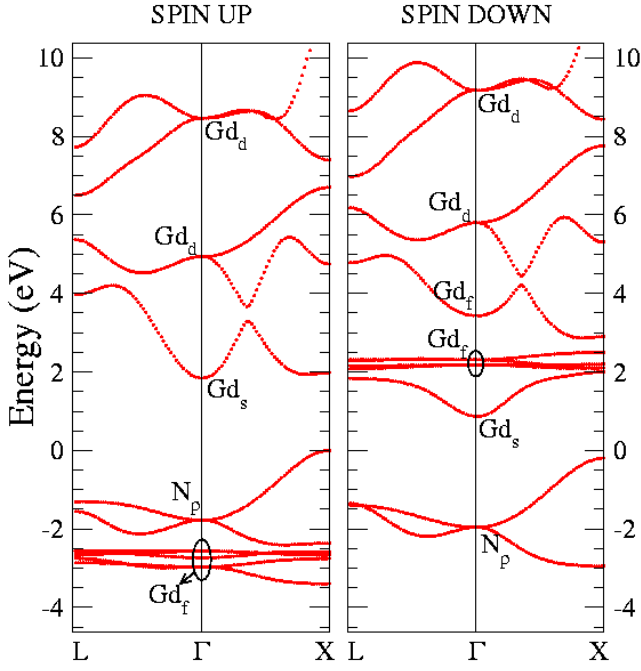


FIG. 1: (Color online) Band structure of the ferromagnetic GdN in the hypothetical zinc-blende structure. The labels indicate the majority character of the band at the  $\Gamma$  point.

## RESULTS AND DISCUSSION

To understand the effect of Gd incorporation in GaN, we first look at the band structure (Fig. 1) of the hypothetical zinc-blende ferromagnetic GdN compound and compare it with that of MnN [14]. We find that in the tetrahedral environment, the crystal field splits the  $f$  orbitals into  $t_1$ ,  $t_2$ , and  $a_1$  states, which can couple to other  $s$ ,  $p$ , and  $d$  states with the same crystal symmetry. For Gd, the majority spin-up  $4f$  states are fully occupied and are below the valence band maximum (VBM) state at  $\Gamma$  with mostly N  $2p$  character and  $t_2$  symmetry. The minority spin-down  $4f$  states are fully unoccupied and are above the conduction band minimum (CBM) at  $\Gamma$ . Unlike the 3d TM, the Gd  $5d$  bands, with  $e$  and  $t_2$  symmetry, are high in energy, and thus are fully unoccupied in the conduction band. The unique position and characters of the Gd  $4f$  and  $5d$  orbitals lead to some unusual features of GdN that are very different from those of Mn-doped GaN. (i) The VBM state at  $\Gamma$ , with  $t_2p$  character, couples strongly with the Gd  $t_{2d}$  and  $t_{2f}$  states. In the spin-up channel, this state is pushed up by the Gd  $t_{2f}$  state below and pushed down by the Gd  $t_{2d}$  state above. In the spin-down channel, this state is pushed down by both the Gd  $t_{2f}$  and  $t_{2d}$  states. However, the  $p$ - $d$  coupling is larger in the spin-up channel, because the potential exchange lowers the spin-up Gd  $t_{2d}$  orbital energy; the net effect is that the exchange splitting at the VBM ( $N_0 = 0.01$  eV) is much smaller than that observed in TM-doped

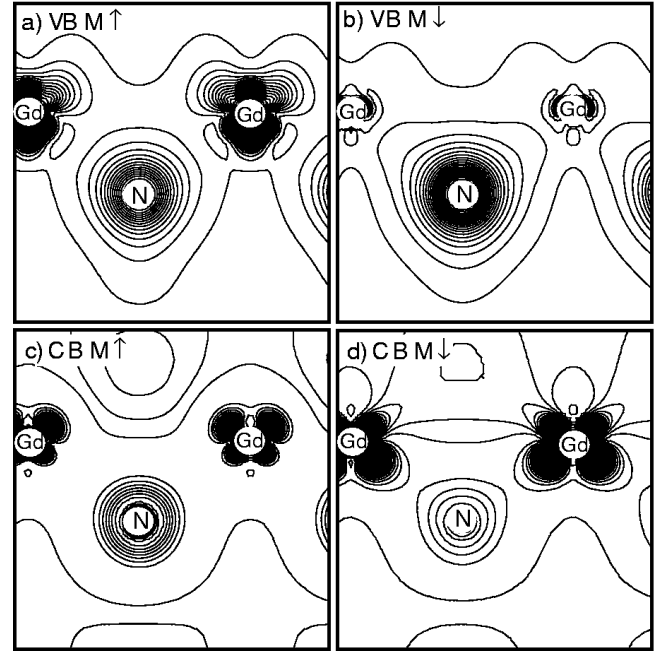


FIG. 2: Wavefunction square of the (a) spin-up VBM, (b) spin-down VBM, (c) spin-up CBM, and (d) spin-down CBM at the zone center.

GaN. Furthermore, because of the strong  $p$ - $d$  coupling at  $\Gamma$ , which pushes the  $t_{2p}$  state down, the top of the valence band is not at  $\Gamma$  as for MnN [14]. (ii) Unlike in TM-doped GaN, where  $s$ - $d$  coupling is not allowed in  $T_d$  symmetry,  $s$ - $f$  coupling is allowed. Because the CBM at  $\Gamma$  has the  $s$  character, in the spin-up channel, it is pushed up by the occupied Gd  $a_{1f}$  state, and in the spin-down channel, it is pushed down by the unoccupied Gd  $a_{1f}$  state. This large kinetic exchange leads to a large negative spin exchange splitting near the CBM ( $N_0 = 0.4$  eV). In contrast, the potential exchange induced splitting in TM-doped GaN is smaller and positive. The wavefunction square of the VBM and CBM states at  $\Gamma$  are plotted in Fig. 2. We see that the spin-up VBM shows a large antibonding  $p$ - $f$  character. The  $f$  character in the spin-down VBM is relatively small because the Gd  $f$  and VBM energy difference is large in the spin-down channel. For the CBM states, we find that the spin-up CBM shows an antibonding  $f$ - $s$  character because the spin-up  $f$  state is below the CBM, whereas the spin-down CBM shows a larger bonding  $f$ - $s$  character because the unoccupied spin-down  $f$  level is above and closer to the CBM. These results are consistent with the energy position and symmetry arguments above.

For diluted GaN Gd magnetic semiconductors, the general features are the same as in pure GdN. The majority Gd  $4f$  orbitals of Gd are always inserted below the VBM of GaN, whereas the minority Gd  $4f$  orbitals are always above the CBM. The Gd  $5d$  orbitals, on the other hand, always have higher energy, above the CBM

of GaN. These features can be seen in Figs. 3 and 4. In Fig. 3 we show the band structure for  $\text{Ga}_{1-x}\text{Gd}_x\text{N}$  with  $x = 0.25$ . Figure 4 shows the density of states (DOS) for  $\text{Ga}_{1-x}\text{Gd}_x\text{N}$  with  $x = 0.0625$ . We observe that the spin-up Gd 4f orbitals are resonant within the valence band with large band widths, whereas the spin-down Gd 4f orbitals are more localized. We can also observe that the DOS at the VBM is very high, indicating a very large valence effective mass in this material. The large valence effective mass comes from the coupling between the VBM and the Gd d orbitals above, which can be seen in Fig. 4. The repulsion between these orbitals pushes the VBM at  $\Gamma$  down, increasing the effective mass. This indicates that this material will have a very small hole mobility. On the other hand, the DOS of the conduction band is very small. This can be understood by the repulsion between the 4f levels and the CBM. This interaction pushes the CBM at  $\Gamma$  down in the spin-down channel, decreasing the electron effective mass. We find that, again, both  $N_0$  and  $N_0'$  are negative for  $\text{Ga}_{1-x}\text{Gd}_x\text{N}$ , with the magnitude of  $N_0'$  much larger than that of  $N_0$ , as can be seen in Fig. 3. This effect is an indication that, for  $\text{Ga}_{1-x}\text{Gd}_x\text{N}$ , the stabilization of ferromagnetism will be more efficient when the carriers are electrons instead of holes.

Because of the highly localized character of the f orbitals, a natural question is whether LSDA can successfully describe the system. Fortunately Gd has a  $4f^7 5d^1 6s^2$  valence configuration, thus it is isovalent with Ga. The majority-spin 4f orbitals are completely filled, whereas the minority-spin 4f orbitals are completely empty. This situation is similar to Mn substituted II-VI diluted semiconductors [15]. The fact that the calculated lattice parameter for GdN is in good agreement with experiment indicates that our LSDA description is reasonable. To further test the adequacy of the LSDA, we have performed general gradient approximation (GGA) [16] and model LDA+U type calculations [15]. We find that besides small quantitative changes (Table I), the qualitative picture described in this paper is unchanged. This can be understood because GGA and LDA+U does not change the f-electron occupation in this system.

Our band structure calculation show that undoped zinc-blende GdN or  $\text{Ga}_{1-x}\text{Gd}_x\text{N}$  alloys [17], are semiconductors because Gd is isovalent to Ga [18]. Our total energy calculations find that undoped GdN and GaGdN in the zinc-blende phase are more stable in the antiferromagnetic phase. The calculated results are shown in Table I for several Gd concentrations  $x$  and configurations. There are always two Gd atoms in the unit cell. These results are expected because no charge carriers are created in this system, therefore, the spin-splitting at the band edge present in the FM phase will not lead to any energy gain compared to the unsplit band edge of the AFM phase. [19] On the other hand, the superexchange coupling between the Gd f states, mediated by the N p

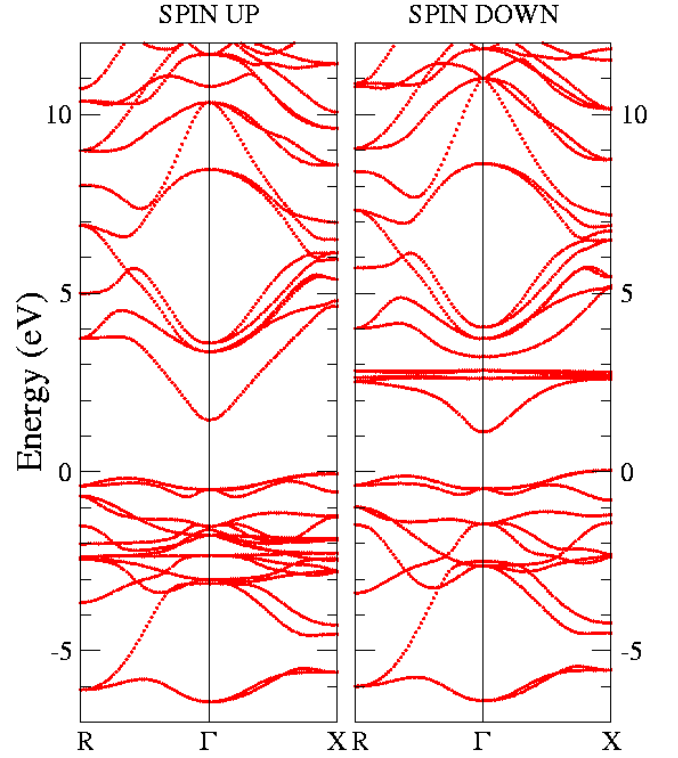


FIG. 3: (Color online) Band structure for the ferromagnetic configuration of  $\text{Ga}_{1-x}\text{Gd}_x\text{N}$  with  $x = 0.25$ .

orbitals, stabilizes the AFM phase. However, compared to TM-doped GaN, the energy differences ( $E_{\text{FM}} - E_{\text{AFM}}$ ) between the FM and AFM states for these systems are small, which is due to the highly localized character of the f orbitals.

In order to stabilize the FM phase, it is necessary to insert carriers into the system. As GaN is usually n-type doped with free electrons in the conduction band [5], we have simulated the effect of donors by introducing electrons into  $\text{Ga}_{1-x}\text{Gd}_x\text{N}$ . In the AFM configuration, the CBM of each spin channel have the same energy, therefore, they will be occupied in both spin channels. In the FM configuration, because of the strong s-f coupling, the CBM has negative spin-exchange splitting, i.e., the spin-down CBM has a lower energy. Consequently, when electrons are added, they will prefer to go to the spin-down CBM of the FM phase, stabilizing the FM configuration. This expectation is supported by our direct total energy calculations of charged systems, where the FM phase becomes more stable. We have considered two different configurations for  $x = 0.125$ , where the Gd atoms are nearest neighbors and next-nearest neighbors. We find that the effective exchange interaction between the two Gd [ $J_{ij}(\mathbf{R})$ ] decreases as the distance between impurities becomes larger.

Several experimental studies [7, 8, 9] of  $\text{Ga}_{1-x}\text{Gd}_x\text{N}$  claim that ferromagnetism is observed up to room tem-

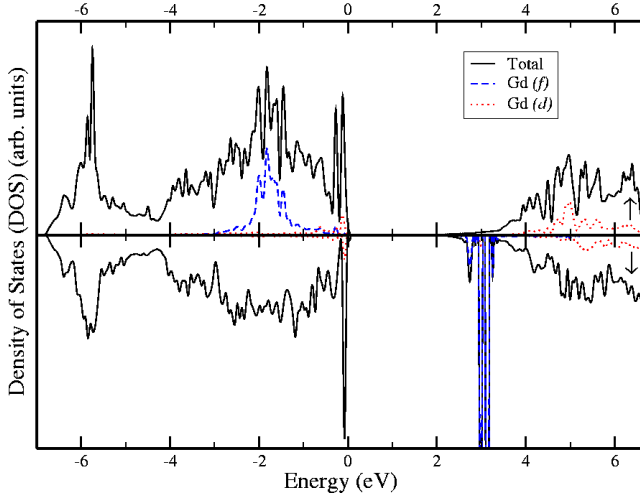


FIG. 4: (Color online) Density of states of  $\text{Ga}_{1-x}\text{Gd}_x\text{N}$  with  $x = 0.0625$ . The blue (dashed) curves are partial DOS of Gd  $f$  levels and the red (dotted) curves are partial DOS of Gd  $d$ . For clarification, the intensity of the DOS related to the Gd  $d$  levels is multiplied by a factor of three.

TABLE I: Energy differences ( $E_{\text{FM}} - E_{\text{AFM}}$ ) between ferromagnetic and antiferromagnetic configurations in  $\text{Ga}_{1-x}\text{Gd}_x\text{N}$ . Energies are in meV; nn and nnn refer to the two Gd atoms as nearest and next-nearest neighbors, respectively, in the unit cell.

$x$	Charge (electrons/Gd)	$E_{\text{FM}} - E_{\text{AFM}}$
1	0	25.0
1	0	22.0 (GGA)
0.25	0	2.6
0.125 (nn)	0	4.4
0.125 (nn)	0.1	-28.4
0.125 (nnn)	0	1.3
0.125 (nnn)	0.1	-19.5

perature. Our calculations show that these observed FM phases should be related to the n-type character of the  $\text{Ga}_{1-x}\text{Gd}_x\text{N}$  samples. This is supported by photoluminescence measurement, which shows the presence of large defect concentration in the sample with FM ordering [20]. A recent measurement also shows that the presence of FM is correlated with Oxygen, a known donor defect in the sample [8], with a concentration of about  $10^{18} \text{ cm}^{-3}$ . These observations are consistent with our model.

One of the unique features observed in Gd-doped GaN is the colossal magnetic moment [8]. It was observed that, at very low Gd concentrations ( $10^{16} \text{ cm}^{-3}$ ), the total effective magnetic moment per Gd atom could be as high as  $4000 \mu_B$ . This is quite unusual because the atomic moment of Gd is only  $8 \mu_B$ , and in the hypothetical zinc-blend GdN the moment per Gd is only  $7 \mu_B$ . When the Gd concentration increases, the effective moments per Gd decrease. This observation was explained

through a phenomenological model, which assumes that Gd atoms polarize the GaN matrix in a certain radius around them and each host atom within the radius has an induced magnetic moment  $p_0$ . Although this model is very interesting and fits experimental results quite well, at least in the low-concentration region, it does not provide a mechanism of the induced magnetic moment. Our band structure calculations above, however, provide a possible explanation of the observed huge magnetic moments: When Gd is introduced into GaN, each Gd introduces unoccupied  $f$  states above the spin-down CBM. The symmetry-allowed coupling between the  $f$  states and states below it can create localized levels with energy below the original CBM. When the system also contains enough shallow donor impurities, as reported in the experiment, two things will occur: (i) the donor electrons of the impurities will occupy the Gd-induced empty levels, if the donor levels of the impurities are higher than the Gd-induced level; (ii) consequently, the system will become ferromagnetic. When enough levels are created by Gd below the donor level, which is possibly due to the symmetry-allowed s-f coupling, the induced magnetic moment per Gd atom can be very high in the extreme impurity limit when the Gd-Gd distances are very large. Translating this into a real-space representation, it is equivalent to say that atoms with a certain radius  $r_0$  around each Gd atom has its spin-down energy levels below the donor levels, and thus they are polarized by the Gd atom with opposite spins. As Gd concentration increases, the spheres surrounding each Gd atom start to overlap. Although some more levels could be pushed below the donor level, thus increasing slightly the effective radius  $r_0$ , eventually the overlap will reduce the effective volume affected by each individual Gd, and therefore, reduce the magnetic moment per Gd, as observed in experiment. However, unlike the previously proposed model, our model has two distinct physical characteristics: (i) To have a large induced magnetic moment, the system must have enough donor impurities; (ii) Our model suggests that the induced magnetic moment has the opposite sign of the Gd magnetic moment. This indicates that when the Gd concentration increases, or the donor carrier density decreases, the magnetic moments in the system will change sign. Experimental testing of our model is called for.

It is interesting to point out that this electron-induced stabilization of ferromagnetic order and large magnetic moments may also occur in TM-doped semiconductors [10]. This is because, despite that s-d coupling is not allowed under  $T_d$  symmetry, it will be allowed when the symmetry of the system is reduced either by strain or by chemical ordering. For example, under (001) strain, the  $a_1(s)$  state can couple to the split  $a_1(e_d)$  state, whereas under (111) strain or in wurtzite crystal, the  $a_1(s)$  state can couple to the split  $a_1(t_d)$  and  $a_1(t_p)$  state. However, in general, the s-d coupling is expected to be smaller than

the symmetry-allowed s-f coupling in these tetrahedral semiconductor systems.

#### SUMMARY

In summary, we have investigated in detail the electronic and magnetic properties of  $Ga_{1-x}Gd_xN$ . We find that because of the coupling between the Gd f and host s states, this system shows some unique behavior that is drastically different from TM-doped GaN. The exchange splitting at the CBM is negative. The coupling between Gd atoms is found to be antiferromagnetic, if no donors are present, but it becomes ferromagnetic when enough donors are present in the system. We also proposed a model that may explain the colossal magnetic moments observed in this system in the very dilute limit, showing that it should be directly related to the polarization of donor electrons.

#### ACKNOWLEDGMENTS

The work at NREL is funded by the U.S. Department of Energy, Office of Science, Basic Energy Sciences, under Contract No. DE-AC36-99GO10337 to NREL.

- 
- [1] I. Zutic, J. Fabian, S. Das Sarma, Rev. Mod. Phys. 76, 323 (2004).
  - [2] D. D. Awschalom and R. K. Kawakami, Nature (London) 408, 923 (2000).
  - [3] T. Dietl, H. Ohno, F. Matsukura, J. Cibert, and D. Fer-  
rand, Science 287, 1019 (2000).

- [4] S. Dhar, O. Brandt, A. Trampert, L. Daweritz, K. J. Friedland, K. H. Ploog, J. Keller, B. Beschoten, and G. Guntherodt, Appl. Phys. Lett. 82, 2077 (2003).
- [5] J. I. Pankove and T. D. Moustakas, Gallium Nitride (GaN) I (Academic, San Diego, 1998).
- [6] D. C. Look, J. W. Hemsky, and J. R. Sizelove, Phys. Rev. Lett. 82, 2552 (1999).
- [7] N. Teraguchi, A. Suzuki, Y. Nanishi, Y.-K. Zhou, M. Hashimoto and H. Aishi, Sol. State Comm. 122, 651 (2002).
- [8] S. Dhar, O. Brandt, M. Ramsteiner, V. F. Sapega, and K. H. Ploog, Phys. Rev. Lett. 94, 037205 (2005).
- [9] H. Aishi, Y. K. Zhou, M. Hashimoto, M. S. Kim, X. J. Li, S. Emura, and S. Hasegawa, J. Phys.: Condens. Matter 16, S5555 (2004).
- [10] J. M. D. Coey, M. Venkatesan, and C. B. Fitzgerald, Nature Materials 4, 173 (2005).
- [11] S.-H. Wei and H. Krakauer, Phys. Rev. Lett. 55, 1200 (1985); D. J. Singh, Planewaves, Pseudopotentials, and the LAPW Method, (Kluwer, Boston, 1994).
- [12] H. J. Monkhorst and J. P. Pack, Phys. Rev. B 13, 5188 (1976).
- [13] D. X. Li, Y. Haga, H. Shida, T. Suzuki, Y. S. Kwon and G. Kido, J. Phys.: Condens. Matter 9, 10777 (1997).
- [14] A. Janotti, S.-H. Wei, and L. Bellaiche, Appl. Phys. Lett. 82, 766 (2003).
- [15] S.-H. Wei and Alex Zunger, Phys. Rev. B 48, 6111 (1993).
- [16] J. P. Perdew and Y. Wang, Phys. Rev. B 45, 13244 (1992).
- [17] H. Hashimoto, S. Emura, R. Asano, H. Tanaka, N. Teraguchi, A. Suzuki, Y. Nanishi, T. Honma, N. Umeshaki, H. Aishi, Phys. Stat. Sol. (c) 0, 2650 (2003).
- [18] W. R. L. Lambrecht, Phys. Rev. B 62, 13538 (2000).
- [19] G. M. Dalpian, S.-H. Wei, X. G. Gong, A. J. R. da Silva, and A. Fazzio, cond-mat/0504084.
- [20] Y. K. Zhou, M. S. Kim, X. J. Li, S. Kimura, A. Kaneta, Y. Kawakami, Sg. Fujita, S. Emura, S. Hasegawa and H. Aishi, J. Phys.: Condens. Matter 16, S5743 (2004).